

Longitudinal PET Monitoring of Amyloidosis and Microglial Activation in a Second Generation Amyloid-beta Mouse Model

Christian Sacher^{1*}, Tanja Blume^{1,2*}, Leonie Beyer^{1*}, Finn Peters², Florian Eckenweber¹, Carmelo Sgobio², Maximilian Deussing¹, Nathalie L. Albert¹, Marcus Unterrainer¹, Simon Lindner¹, Franz-Josef Gildehaus¹, Barbara von Ungern-Sternberg¹, Irena Brzak³, Ulf Neumann³, Takashi Saito⁴, Takaomi C. Saido⁴, Peter Bartenstein¹, Axel Rominger^{1,5,6}, Jochen Herms^{2,5,7*}, Matthias Brendel^{1,5*}

¹Dept. of Nuclear Medicine, University Hospital of Munich, LMU Munich, Munich Germany

²DZNE - German Center for Neurodegenerative Diseases, Munich, Germany

³Neuroscience, Novartis Institutes for BioMedical Research (NIBR), Basel, Switzerland

⁴Laboratory for Proteolytic Neuroscience, RIKEN Center for Brain Science, Saitama, Japan

⁵Munich Cluster for Systems Neurology (SyNergy), Munich, Germany

⁶Department of Nuclear Medicine, Inselspital, University Hospital Bern, Bern, Switzerland.

⁷Center of Neuropathology and Prion Research, University of Munich, Germany

*Contributed equally

11/05/2019

Short title: Micro-PET in *App*^{NL-G-F} mice

Key words: Alzheimer's disease; β -amyloid; microglia; *App*^{NL-G-F}; spatial learning

Word count: 4996

Corresponding author:

Matthias Brendel MD; Department of Nuclear Medicine; LMU Munich, Germany; Phone:+49(0)89440074650; Fax:+49(0)89440077534; E-Mail: matthias.brendel@med.uni-muenchen.de

First author:

Christian Sacher (medical student); Department of Nuclear Medicine; LMU Munich, Germany; Phone:+49(0)1623878661; E-Mail: christian.sacher@med.uni-muenchen.de

1 **ABSTRACT**

2 *Aim:* Non-physiological overexpression of β -amyloid ($A\beta$) precursor protein
3 in common transgenic $A\beta$ mouse models of Alzheimer's disease (AD) likely
4 hampers their translational potential. The novel App^{NL-G-F} mouse incorporates a
5 mutated knock-in, potentially presenting an improved model of AD for $A\beta$ -
6 targeting treatment trials. We aimed to establish serial small animal positron-
7 emission-tomography (μ PET) of amyloidosis and neuroinflammation in App^{NL-G-F}
8 mice as a tool for therapy monitoring.

9 *Methods:* App^{NL-G-F} mice (homozygous $n=20$; heterozygous $n=21$) and
10 age-matched wild-type mice ($n=12$) were investigated longitudinally from 2.5 to
11 10 months of age with ^{18}F -florbetaben $A\beta$ - μ PET and ^{18}F -GE-180 18kDa
12 translocator protein (TSPO)- μ PET. Voxel-wise analysis of standardized-uptake-
13 value-ratios (SUVR) images was performed using statistical parametric mapping.
14 All mice underwent a Morris water maze test of spatial learning after their final
15 μ PET scan. Quantification of fibrillar $A\beta$ and activated microglia by
16 immunohistochemistry and biochemistry served for validation of μ PET results.

17 *Results:* The periaqueductal gray emerged as a suitable pseudo-
18 reference tissue for both tracers. Homozygous App^{NL-G-F} mice had rising SUVR in
19 cortex and hippocampus for $A\beta$ - (+9.1%, +3.8%) and TSPO- (+19.8%, +14.2%)
20 μ PET from 2.5 to 10 months of age (all $p < 0.05$), whereas heterozygous App^{NL-G-}
21 F mice did not show significant changes with age. Significant voxel-wise clusters
22 of $A\beta$ deposition and microglial activation in homozygous mice appeared at five
23 months of age. Immunohistochemical and biochemical findings correlated

1 strongly with μ PET data. Water maze escape latency was significantly elevated
2 in homozygous App^{NL-G-F} mice compared to wild-type at ten months of age and
3 was associated with high TSPO binding.

4 *Conclusion:* Longitudinal μ PET in App^{NL-G-F} knock-in mice enables
5 monitoring of amyloidogenesis and neuroinflammation in homozygous mice, but
6 is insensitive to minor changes in heterozygous animals. The combination of
7 μ PET with behavioral tasks in App^{NL-G-F} treatment trials is poised to provide
8 important insights in preclinical drug development.

9

1 INTRODUCTION

2 Alzheimer's disease (AD) is the most common neurodegenerative disease, with
3 an incidence that increases exponentially with age, such that the prevalence
4 exceeds 10% among octagenarians and 30% for nonagenarians. This epidemic
5 is placing a growing socioeconomic burden on health care in societies with aging
6 populations (1). The neuropathology of AD classically includes the accumulation
7 of amyloid- β peptide ($A\beta$) as extracellular plaques, and fibrillary tau aggregates
8 within neurons. Activation of multiple neuroinflammatory pathways mediated by
9 activated microglia expressing high levels of the marker 18-kDa translocator
10 protein (TSPO) completes the triad of markers. These pathologies, mainly
11 restricted to the cerebral cortex and the hippocampus, lead to a progressive
12 decline in cognitive function, usually first manifesting with memory complaints (2-
13 6). The identification of familial AD mutations in the amyloid precursor protein
14 (APP) gene has led to the generation of a number of transgenic mouse models
15 that overexpress APP (7,8). These first-generation mouse models exhibit AD
16 pathology, but the non-physiological overexpression of APP may cause
17 additional phenotypes unrelated to AD. To circumvent these intrinsic drawbacks,
18 second-generation APP knock-in mice that carry pathogenic mutations in the
19 APP gene have been established (9). For example, *App*^{NL-G-F} mice carry a mutant
20 APP gene encoding the humanized $A\beta$ sequence (G601R, F606Y, and R609H)
21 with three pathogenic mutations, namely Swedish (KM595/596NL),
22 Beyreuther/Iberian (I641F), and Arctic (E618G). Homozygotic *App*^{NL-G-F} mice
23 progressively exhibit widespread $A\beta$ accumulation along with activation of

1 microglia and astrocytes from two months of age, and express behavioral
2 symptoms in the form of declining spatial learning ability from eight to 12 months
3 of age (10-13). Given their physiological expression of APP in comparison to
4 transgenic mouse models, these knock-in mice are not characterized by
5 massively elevated expression of the intracellular domain of APP or soluble
6 APP α (9). Therefore, this mouse model potentially avoids confounds due to non-
7 physiological signaling in therapy testing trials.

8 Previous studies have shown that small animal positron-emission tomography
9 (μ PET) is a suitable non-invasive tool for monitoring of therapeutic trials targeting
10 AD pathology (14,15). We previously established μ PET for monitoring of A β
11 deposition and microglial activation in APP-overexpressing mice, yielding
12 excellent correlations with histological and biochemical assessments (16). Given
13 this background, the aim of this study was to transfer μ PET methodology to the
14 *App^{NL-G-F}* mouse model in a longitudinal investigation of the amyloid tracer ^{18}F -
15 florbetaben (^{18}F -FBB) and the TSPO tracer ^{18}F -GE-180. We confirmed the new
16 dual tracer μ PET results relative to findings obtained by immunohistochemistry
17 and biochemistry and correlated the neuropathology findings with scores in a test
18 of spatial learning.

19

20 **MATERIALS AND METHODS**

21 **Animals and Study Design**

22 All experiments were performed in compliance with the National Guidelines for
23 Animal Protection, Germany with the approval of the regional animal committee
24 (Regierung Oberbayern) and were overseen by a veterinarian. Animals were

1 housed in a temperature- and humidity-controlled environment with 12 h light-
2 dark cycle, with free access to food (Sniff, Soest, Germany) and water. The
3 experiments were carried out in mixed sex groups of heterozygous (n=21) and
4 homozygous (n=20) *App^{NL-G-F}* mice, which is a knock-in mouse line generated by
5 Saito and colleagues (11), and a group of age-matched wild-type mice. μ PET
6 examinations (A β and TSPO) were performed in a longitudinal design at baseline
7 (2.5 months of age) and three follow-up measurements (5.0, 7.5 and 10.0
8 months). Serial μ PET scans of both tracers deriving from a total of 12 age- and
9 sex-matched wild-type mice served as controls, in consideration of the age-
10 dependent increase of cortical TSPO- μ PET signal in wild-type mice (17). All
11 available mice underwent Morris water maze tests within two weeks after their
12 final μ PET scan. After behavioral testing, mice were deeply anaesthetized prior
13 to transcardial perfusion and brain extraction. A minimum number of four brains
14 per genotype were processed for immunohistochemistry and biochemistry in
15 randomly selected hemispheres.

17 **μ PET Imaging**

18 *μ PET Data Acquisition, Reconstruction and Post-Processing:* For all μ PET
19 procedures, we used an established standardized protocol for radiochemistry,
20 acquisition and pre-processing (16). In brief, ^{18}F -GE-180 TSPO- μ PET (13.4 ± 1.6
21 MBq; ~ 400 -1400 GBq/ μmol) recordings with an emission window of 60-90 min
22 p.i. were obtained to measure cerebral TSPO expression, along with ^{18}F -FBB A β -
23 μ PET (12.9 ± 1.7 MBq; ~ 30 -80 GBq/ μmol) recordings with an emission window of

1 30-60 min p.i. for assessment of fibrillar cerebral amyloidosis. Two *App*^{NL-G-F} mice
2 aged eleven months were imaged in a dynamic setting (¹⁸F-FBB: 0-60 min p.i.;
3 ¹⁸F-GE-180: 0-90 min p.i.) and their results compared to historic dynamic wild-
4 type data for validation of the previously established time windows in this model.
5 Anesthesia was maintained from just prior to tracer injection to the end of the
6 imaging time window.

7 *μPET Image Analysis:* We performed all analyses using PMOD (V3.5, PMOD
8 technologies, Basel, Switzerland). First, intensity normalization of images to
9 standardized-uptake-value (SUV) images was conducted by the previously
10 validated myocardium correction method (18) for TSPO-μPET (SUV_{MC}) and by
11 conventional SUV calculation for Aβ-μPET. Voxel-based comparisons of SUV
12 images between *App*^{NL-G-F} (n=13 per tracer, 10 months) and wild-type mice (n=6
13 per tracer, ten months) were performed to investigate a suitable pseudo-
14 reference tissue for μPET quantification in the *App*^{NL-G-F} mouse model. The
15 judgment of suitability was also informed by the immunohistochemistry results
16 described below. A suitable pseudo-reference tissue was defined as a brain
17 region lacking any genotypic difference in μPET and immunohistochemistry
18 results for both radioligands. These criteria lead us to select the mesencephalic
19 periaqueductal gray (PAG, comprising 20 mm³) as pseudo-reference region for
20 calculation of SUV-ratio (SUVR) values for both Aβ-μPET and TSPO-μPET (Fig.
21 1). Two bilateral frontal cortical (CTX) target volumes-of-interest (VOIs,
22 comprising 24 mm³ each) and two bilateral hippocampal (HIP) target VOIs
23 (comprising 10 mm³ each) were used for both tracers. Target-to-reference tissue

1 SUVRs were calculated for cortex (SUVR_{CTX/PAG}) and hippocampus
2 (SUVR_{HIP/PAG}) for A β - and TSPO- μ PET.

3 *SPM Analysis:* For both tracers, whole-brain voxel-wise comparisons of PAG-
4 scaled SUVR images between groups of knock-in and wild-type mice were
5 performed as described previously (19, 20).

6

7 **Behavioral Testing**

8 Mice (homozygous *App*^{NL-G-F}: n=11, heterozygous *App*^{NL-G-F}: n=14, wild-type:
9 n=3) underwent a Morris water maze test for spatial learning and memory
10 deficits, which was performed according to a standard protocol with small
11 adjustments (21). The video tracking software EthoVision® XT (Noldus) was used
12 for analyses of escape latency during the training period as well as at the probe
13 trial.

14

15 **Immunohistochemistry and Biochemistry**

16 In brain regions corresponding to μ PET VOIs (for details see also Supplemental
17 Table 1), histochemistry was performed for fibrillar A β (methoxy-X04, TOCRIS)
18 and immunohistochemistry for activated microglia using an Iba1 primary antibody
19 (Wako) as previously established (17,22). NAB228 (Santa Cruz) was used for
20 immunohistochemistry labelling of fibrillar as well as non-fibrillar A β depositions.
21 Hemispheres from five homozygous *App*^{NL-G-F}, five heterozygous *App*^{NL-G-F} and
22 four wild-type mice were used for immunohistochemistry. Assessment of A β 40
23 and A β 42 was performed as previously described (23). Biochemical analyses

1 were performed in samples from the entire forebrain. Soluble Trem2 protein was
2 extracted from brain tissue with Tris-buffered saline, and measured by ELISA,
3 using polyclonal sheep antibody for coating (AF1729, R&D Systems) and
4 biotinylated polyclonal sheep antibody (BAF1729, R&D Systems) together with
5 streptavidin-horseradish peroxidase (N-100 ThermoFisher Scientific) for
6 detection. Hemispheres from eight homozygous *App^{NL-G-F}*, 14 heterozygous
7 *App^{NL-G-F}* and four wild-type were used for biochemical analyses.

8

9 **Statistics**

10 Group comparisons of VOI-based μ PET results between knock-in and wild-type
11 mice were performed by one-way ANOVA and Tukey *post hoc* test for multiple
12 comparisons, calculated by IBM SPSS 25 Statistics (IBM Deutschland GmbH,
13 Ehningen, Germany). Two-sided t-tests were used to compare terminal
14 multimodal readouts of homozygous *App^{NL-G-F}* with wild-type or heterozygous
15 *App^{NL-G-F}* groups. Two-way ANOVA was applied to assess methoxy-X04 and
16 NAB228 fluorescence intensity changes distant and close to plaques. For
17 correlation analyses in *App^{NL-G-F}*, Pearson's coefficients of correlation (R) were
18 calculated for normally distributed readouts after Kolmogorov-Smirnov testing for
19 normalcy. For non-normally distributed readouts, Spearman's coefficients of
20 correlation (r_s) were calculated. A threshold of $p < 0.05$ was considered significant
21 for rejection of the null hypothesis. Sample size calculations for potential
22 upcoming treatment trials were performed for longitudinal (2.5 to 10.0 months)
23 and terminal measures in the cortical VOI for both ligands in homozygous *App^{NL-}*

1 $G-F$ mice. We used a simplified t -statistic model with assumptions of a type I error
2 $\alpha=0.05$, a power of 0.8 and a treatment effect of 50% calculated in G*Power
3 (V3.1, Heinrich-Heine University, Duesseldorf, Germany). For the power
4 calculation we simulated the treatment group by calculating longitudinal
5 differences within single App^{NL-G-F} mice and terminal differences of single App^{NL-}
6 $G-F$ by multiplying the mean endpoint of wild-type for each tracer by 0.5,
7 corresponding to the 50% treatment effect.

8

9 **RESULTS**

10 **Pseudo Reference Region**

11 Immunohistochemistry revealed a widespread amyloidosis and microglial
12 activation in App^{NL-G-F} mice at ten months of age, involving most regions of the
13 forebrain (Fig. 1). Regions with relatively low amyloidosis and microglial
14 activation were observed in parts of the hindbrain, i.e. vermis, midbrain, and
15 notably the PAG. SUV differences between genotypes at ten months of age fitted
16 to immunohistochemistry and revealed lowest ^{18}F -FBB and ^{18}F -GE180
17 alterations in the hindbrain (Fig. 1). SUV analysis at the final time point revealed
18 that an oval shaped VOI primarily composed of PAG voxels yields a suitable
19 pseudo-reference region (^{18}F -FBB SUV: App^{NL-G-F} : 0.47 ± 0.08 , wild-type: $0.46 \pm$
20 0.09 , n.s. / ^{18}F -GE180 SUV_{MC}: App^{NL-G-F} : 0.22 ± 0.02 , wild-type: 0.23 ± 0.02 ,
21 n.s.). SUVR_{CTX/PAG} time-activity-curves of aged App^{NL-G-F} mice revealed stable
22 uptake differences for 30-60 min p.i. ^{18}F -FBB and 60-90 min p.i. ^{18}F -GE180
23 imaging when compared to historic wild-type data (Supplemental Fig. 1).

Furthermore, the comparison of methoxy-X04 and NAB228 staining revealed only a minor fraction of fibrillar A β in amyloid plaques in the entire brain (Fig. 2), which predicted a relatively lower ^{18}F -FBB signal when compared to historically investigated amyloid mouse models.

Dual Tracer μPET Analyses

A comprehensive overview of μPET results is provided in Table 1. The age dependence of the retention of the two tracers is presented in Fig. 3 and illustrated in Supplemental Fig. 2. The voxel-based approach is presented and discussed in the Supplement including Supplemental Fig. 3.

A β - μPET Findings: homozygous *App*^{NL-G-F} mice already showed elevated cortical ^{18}F -FBB SUVR compared to their baseline as early as five months of age (+3.4%; $p < 0.05$), which had increased further at ten months (+9.1%; $p < 0.001$). Hippocampal increases of SUVR first became apparent at 7.5 months (+2.6%; $p < 0.05$) and were more conspicuous at ten months (+3.8%; $p < 0.001$). Required sample sizes for detection of a 50% A β - μPET treatment effect in the cortex of homozygous *App*^{NL-G-F} mice were $n=11$ for evaluation of longitudinal measures between 2.5 and 10 months and $n=8$ for the terminal time-point. The heterozygous genotype did not show significant changes in ^{18}F -FBB SUVR relative to baseline at any age.

TSPO- μPET Findings: homozygous *App*^{NL-G-F} mice revealed the first evidence of increased cortical ^{18}F -GE-180 uptake compared to baseline as early as five months (+6.5%; $p < 0.05$), which increased strongly by ten months (+19.8%;

1 p<0.001). Significantly elevated ^{18}F -GE-180 SUVR in the hippocampus was
2 present at 7.5 months (+10.8%; p<0.001), which increased further by ten months
3 (+14.2%; p<0.001). Required sample sizes for detection of a 50% TSPO- μ PET
4 treatment effect in the cortex of homozygous *App*^{NL-G-F} mice were n=16 for
5 evaluation of longitudinal measures between 2.5 and 10 months and n=11 for the
6 terminal time-point. The heterozygous genotype revealed neither cortical nor
7 hippocampal microglial activation at any age.

8 *Correlation Analyses:* Significant positive associations between A β and TSPO-
9 μ PET quantification were observed for the cortex (R=0.64; p<0.001; Fig. 3C) and
10 the hippocampus (R=0.48; p<0.05; Fig. 3F).

11

12 **Correlation with Multimodal Terminal Readouts**

13 Average values for the different genotypes of all terminal readouts at the age of
14 ten months are presented in Supplemental Table 1. We observed strong
15 increases in all biochemical (A β 40, A β 42, sTrem2) and (immuno)histochemistry
16 (Iba1, methoxy-X04; see Supplemental Fig. 4) readouts in the comparison of
17 homozygous *App*^{NL-G-F} with wild-type or heterozygous *App*^{NL-G-F} animals. Spatial
18 learning score was substantially impaired in the homozygous *App*^{NL-G-F} compared
19 to wild-type groups (latency to platform +2.1-fold, p<0.05, two-tailed), with no
20 such difference for heterozygous *App*^{NL-G-F}. All correlations between SUVRs at
21 ten months of age and multimodal terminal readouts are illustrated in Fig. 4.

22 *Biochemistry:* A β 42 concentration correlated highly with cortical ^{18}F -FBB
23 (r_s =0.69; p<0.001) and ^{18}F -GE-180 uptake (r_s =0.70; p<0.001). Furthermore,

1 significant A β 42 correlations with hippocampal SUVRs were observed for both
2 tracers ($p < 0.01$). Quantification of sTrem2 correlated with cortical ($r_s = 0.61$;
3 $p < 0.01$) and hippocampal ($r_s = 0.53$; $p < 0.05$) SUVR of ^{18}F -GE-180.
4 *Immunohistochemistry*: Hippocampal ($r_s = 0.90$; $p < 0.001$) and cortical ($R = 0.75$;
5 $p < 0.05$) ^{18}F -FBB uptake was strongly correlated with plaque burden, measured
6 by methoxy-X04 histology in the corresponding regions. The Iba1 burden, which
7 is indicative of activated microglia, correlated with uptake of the TSPO tracer ^{18}F -
8 GE-180 in neocortex ($R = 0.92$; $p < 0.001$) and hippocampus ($R = 0.78$; $p < 0.01$).
9 *Behavioral Analysis*: There was a moderate significant association between
10 cortical ^{18}F -GE-180 SUVR and escape latency at ten months ($R = 0.41$; $p < 0.05$),
11 meaning that mice with stronger microglial activation needed significantly more
12 time to reach the platform in the Morris water maze test.

13

14 **DISCUSSION**

15 This is the first longitudinal dual-tracer μPET study of cerebral amyloidosis
16 and neuroinflammation in a knock-in AD mouse model. After modification of
17 standardized μPET protocols to circumvent model-specific difficulties in
18 homozygous *App*^{NL-G-F} knock-in mice, we detected strong progressive increases
19 of ^{18}F -FBB and ^{18}F -GE-180 uptake with age. Terminal validation analyses by
20 immunohistochemistry and biochemistry confirmed these *in vivo* μPET results.
21 The present findings establish the basis for serial μPET monitoring of therapeutic
22 agents targeting A β deposition and microglial activation in *App*^{NL-G-F} mice.

23 Two model-specific issues were encountered and solved for establishing

1 μ PET imaging in *App*^{NL-G-F} mice: First, the widespread amyloid pathology in brain
2 hampered the use of previously established reference regions such as the
3 cerebellum or white matter (16). SUVR scaling by an appropriate intracerebral
4 reference tissue represents an important tool to generate robust μ PET results
5 during short acquisition times in mice. This is crucial for the present *App*^{NL-G-F}
6 model mice, which are vulnerable to more stress-related drop-outs compared to
7 other amyloid mouse models (10). While full kinetic modelling with arterial blood
8 sampling represents the gold standard for μ PET quantification, that approach is
9 hardly feasible in mouse studies encompassing up to four pairs of μ PET
10 sessions. Therefore, we made use of a variance analysis for both μ PET tracers
11 together with immunohistochemistry assessment to identify the most valid
12 pseudo-reference tissue, which proved to be PAG of the mesencephalon.
13 Validation in serial dual μ PET imaging revealed robust quantification of SUVR
14 relative to PAG, and terminal assessments substantiated our use of this pseudo-
15 reference tissue through the excellent correlation of terminal μ PET results with
16 immunohistochemistry gold standards. A low dropout rate during serial μ PET
17 imaging (<10% per time-point) also encourage the use of our newly established
18 SUVR protocol. We note that the range SUVR fell below unity for quantification of
19 both tracers, due to higher unspecific binding in the PAG reference tissue when
20 compared to cortical or hippocampal target regions. Using the reference tissue
21 normalization, but reducing variance in the population, stabilized PET
22 quantification, just as in our previous investigations of both ligands (16,24).

23 Another aspect of the present model concerns the fraction of dense

1 fibrillar A β in the plaques of *App*^{NL-G-F} mice, which is lower than in other
2 transgenic amyloid mouse models. This is an important technicality, as
3 fluorinated A β - μ PET tracers such as ¹⁸F-FBB have high affinity for dense fibrillary
4 plaques, but exhibit only low binding in diffuse plaques (25). As expected from
5 this, we observed a lesser longitudinal increase for ¹⁸F-FBB binding when
6 compared to ¹⁸F-GE-180 from the plaque onset until the full blown pathology
7 occurring at ten months of age (9.1% vs. 19.8%). In contrast, we had earlier
8 found similar increases of the same two radioligands in APP-SL70 (18.3% vs.
9 17.6%) (26) and PS2APP mice (+19.8% vs. +20.2%) (16). Thus, while
10 quantitative β -amyloid imaging to ¹⁸F-FBB μ PET is feasible in *App*^{NL-G-F} mice, the
11 tracer misses at least half of the true plaque burden, which constitutes a
12 weakness of using this particular radioligand in the knock-in mouse model. This
13 property needs to be addressed in future studies of A β -targeting therapies or
14 genetic modifications with differential effects on the expressions of dense and
15 diffuse parts of the plaque (27).

16 Serial μ PET analyses and terminal assessments of our study indicated
17 parallel increases of amyloidosis and microglial activation with age in the
18 transgenic knock-in mice. The observed strong correlations between cortical
19 TSPO and A β readouts were expected from results of a published study, which
20 demonstrated a link between amyloidosis and neuroinflammation based on
21 comparative profiling of cortical gene expression in AD patients and in the *App*^{NL-}
22 ^{G-F} mouse model (13). Our recent study of PS2APP mice showed that the
23 concentration of sTrem2, which is expressed by microglia as a mediator of

1 phagocytic clearance of debris (6), is highly correlated with TSPO and A β μ PET
2 signals (28). The present biochemical analysis of sTrem2 also showed strong
3 correlations with terminal TSPO- μ PET, but not with A β - μ PET. This may indicate
4 that sTrem2 serves as a valid biomarker for microglial activation in *App^{NL-G-F}*
5 mice, but its expression not so tightly coupled to fibrillar A β levels in *App^{NL-G-F}*
6 mice when compared to PS2APP mice.

7 Spatial learning performance at ten months of age (also discussed in the
8 Supplement) did not correlate with longitudinal A β - μ PET, nor with terminal
9 immunohistochemistry or biochemical measures of amyloidosis, which is in line
10 with a recent review of different transgenic mouse models of AD (29). Our
11 previous study with TSPO- μ PET in PS2APP revealed some evidence for an
12 association between consistently strong early and terminal neuroinflammation
13 with a better preservation of cognitive function (30), suggesting a net protective
14 effect of microglial activation. In contrast, the deterioration in spatial learning in
15 aged *App^{NL-G-F}* mice correlated significantly with increased cortical TSPO- μ PET
16 SUVR at the terminal time point. With regard to the specific plaque composition
17 observed in *App^{NL-G-F}*, which has less dense but more diffuse plaques in
18 comparison to first generation amyloid mouse models, present findings call for
19 further examination of the specific role of microglial activation in *App^{NL-G-F}*
20 neuropathology. Furthermore, we should in future consider applying other
21 behavioral assessment in addition to the Morris water maze test of spatial
22 learning. Inter-mouse-model comparisons of findings from imaging in conjunction
23 with other biomarkers are summarized in Supplemental Table 2.

Molecular imaging with μ PET uniquely affords longitudinal monitoring of disease-related alterations and interventions in individual animals, and can allow prediction of progression and therapeutic effects from early baseline characteristics (14,15). Recent therapeutic studies in transgenic mouse models monitored by PET, for instance using an inhibitor of the β -site amyloid precursor protein-cleaving enzyme 1 (BACE1), have already shown encouraging results with respect to delayed pathology (14,31,32). Our serial *in vivo* μ PET results together with *ex vivo* observations in *App^{NL-G-F}* mice, representing an aggressively neurotoxic knock-in amyloid model with cognitive impairment, support the use of these methods for interventional studies, especially when fibrillary parts of the plaque are targeted by the therapy, as is especially relevant for anti-amyloid antibodies.

CONCLUSION

Analysis of A β - and TSPO- μ PET imaging in *App^{NL-G-F}* mice is complicated by the widespread cerebral pathology and relatively low fibrillarity of A β plaques, but is feasible using PAG as a pseudo-reference region. Progression of neuropathology can be tracked by serial ^{18}F -FBB and ^{18}F -GE-180 μ PET in homozygous *App^{NL-G-F}* mice, whereas heterozygous *App^{NL-G-F}* animals present only minor changes to these methods. The combination of μ PET with a test of cognition in this new knock-in AD model *App^{NL-G-F}* is a promising test-bed for preclinical drug development.

1 **Acknowledgements**

2 We thank Karin Bormann-Giglmaier for excellent technical assistance.
3 Florbetaben precursor was provided by Life Molecular. GE made GE-180
4 cassettes available through an early access model. We acknowledge Inglewood
5 Biomedical Editing for manuscript editing. Seed funding was provided by Verein
6 zur Förderung von Wissenschaft und Forschung an der Medizinischen Fakultät
7 der Ludwig-Maximilians-Universität München. This work was supported by the
8 Deutsche Forschungsgemeinschaft (DFG) by a grant to M.B.&A.R. (BR4580/1-
9 1&RO5194/1-1) and within the framework of the Munich Cluster for Systems
10 Neurology (EXC1010SyNergy).

11

12 **Conflict of Interest**

13 PB&AR received speaking honoraria from Life Molecular, IB&UN are employees
14 of Novartis. All other authors report no conflicts

15

1 **KEY POINTS**

2 QUESTION: Is it possible to monitor preclinical trials using amyloid precursor
3 protein (APP) knock-in mice by means of small animal positron-emission-
4 tomography (PET) for β -amyloid and 18kDa translocator protein?

5 PERTINENT FINDINGS: This longitudinal preclinical investigation revealed
6 progressively increasing uptake of PET tracers for β -amyloid and 18kDa
7 translocator protein in APP knock-in mice. Terminal PET findings were highly
8 correlated with ex vivo gold standard assessments.

9 TRANSLATIONAL IMPLICATIONS: PET in APP knock-in mice present a new
10 instrument for bench to bedside therapy monitoring without interference from
11 APP overexpression.

12

References

1. Ziegler-Graham K, Brookmeyer R, Johnson E, Arrighi HM. Worldwide variation in the doubling time of Alzheimer's disease incidence rates. *Alzheimers Dement.* 2008;4:316-323.
2. Braak H, Braak E. Demonstration of amyloid deposits and neurofibrillary changes in whole brain sections. *Brain Pathol.* 1991;1:213-216.
3. Hyman BT, Phelps CH, Beach TG, et al. National Institute on Aging-Alzheimer's Association guidelines for the neuropathologic assessment of Alzheimer's disease. *Alzheimers Dement.* 2012;8:1-13.
4. Serrano-Pozo A, Frosch MP, Masliah E, Hyman BT. Neuropathological alterations in Alzheimer disease. *Cold Spring Harb Perspect Med.* 2011;1:a006189.
5. Querfurth HW, LaFerla FM. Alzheimer's disease. *N Engl J Med.* 2010;362:329-344.
6. Heneka MT, Carson MJ, Khoury JE, et al. Neuroinflammation in Alzheimer's disease. *Lancet Neurol.* 2015;14:388-405.

- 1 **7.** Jonsson T, Atwal JK, Steinberg S, et al. A mutation in APP protects
2 against Alzheimer's disease and age-related cognitive decline. *Nature*.
3 2012;488:96-99.
- 4
- 5 **8.** Hsiao K, Chapman P, Nilsen S, et al. Correlative memory deficits, Abeta
6 elevation, and amyloid plaques in transgenic mice. *Science*. 1996;274:99-102.
- 7
- 8 **9.** Sasaguri H, Nilsson P, Hashimoto S, et al. APP mouse models for
9 Alzheimer's disease preclinical studies. *EMBO J*. 2017;36:2473-2487.
- 10
- 11 **10.** Masuda A, Kobayashi Y, Kogo N, Saito T, Saido TC, Itohara S. Cognitive
12 deficits in single App knock-in mouse models. *Neurobiol Learn Mem*.
13 2016;135:73-82.
- 14
- 15 **11.** Saito T, Matsuba Y, Mihira N, et al. Single App knock-in mouse models of
16 Alzheimer's disease. *Nat Neurosci*. 2014;17:661-663.
- 17
- 18 **12.** Sakakibara Y, Sekiya M, Saito T, Saido TC, Iijima KM. Cognitive and
19 emotional alterations in App knock-in mouse models of Abeta amyloidosis. *BMC*
20 *Neurosci*. 2018;19:46.

21

- 1 **13.** Castillo E, Leon J, Mazzei G, et al. Comparative profiling of cortical gene
2 expression in Alzheimer's disease patients and mouse models demonstrates a
3 link between amyloidosis and neuroinflammation. *Sci Rep.* 2017;7:17762.
4
- 5 **14.** Brendel M, Jaworska A, Overhoff F, et al. Efficacy of chronic BACE1
6 inhibition in PS2APP mice depends on the regional Abeta deposition rate and
7 plaque burden at treatment initiation. *Theranostics.* 2018;8:4957-4968.
8
- 9 **15.** Brendel M, Jaworska A, Herms J, et al. Amyloid-PET predicts inhibition of
10 de novo plaque formation upon chronic γ -secretase modulator treatment. *Mol*
11 *Psychiatry.* 2015;20:1179-1187.
12
- 13 **16.** Brendel M, Probst F, Jaworska A, et al. Glial activation and glucose
14 metabolism in a transgenic amyloid mouse model: A triple-tracer PET Study. *J*
15 *Nucl Med.* 2016;57:954-960.
16
- 17 **17.** Brendel M, Focke C, Blume T, et al. Time courses of cortical glucose
18 metabolism and microglial activity across the life span of wild-type mice: A PET
19 study. *J Nucl Med.* 2017;58:1984-1990.
20
- 21 **18.** Deussing M, Blume T, Vomacka L, et al. Coupling between physiological
22 TSPO expression in brain and myocardium allows stabilization of late-phase
23 cerebral [(18)F]GE180 PET quantification. *Neuroimage.* 2018;165:83-91.

1
2
3
4
5
6
7
8
9
10
11
12
13
14
15
16
17
18
19
20
21
22

19. Rominger A, Brendel M, Burgold S, et al. Longitudinal assessment of cerebral b-amyloid deposition in mice overexpressing Swedish mutant b-amyloid precursor protein using 18F-florbetaben PET. *J Nucl Med.* 2013;54:1127-1134.

20. Sawiak SJ, Wood NI, Williams GB, Morton AJ, Carpenter TA. Voxel-based morphometry in the R6/2 transgenic mouse reveals differences between genotypes not seen with manual 2D morphometry. *Neurobiol Dis.* 2009;33:20-27.

21. Bromley-Brits K, Deng Y, Song W. Morris water maze test for learning and memory deficits in Alzheimer's disease model mice. *J Vis Exp.* 2011. 2011;53:e2920

22. Dorostkar MM, Dreosti E, Odermatt B, Lagnado L. Computational processing of optical measurements of neuronal and synaptic activity in networks. *J Neurosci Methods.* 2010;188:141-150.

23. Neumann U, Rueeger H, Machauer R, et al. A novel BACE inhibitor NB-360 shows a superior pharmacological profile and robust reduction of amyloid-beta and neuroinflammation in APP transgenic mice. *Mol Neurodegener.* 2015;10:44.

- 1 **24.** Overhoff F, Brendel M, Jaworska A, et al. Automated spatial brain
2 normalization and hindbrain white matter reference tissue give improved [18F]-
3 florbetaben PET quantitation in Alzheimer's model mice. *Front Neurosci.*
4 2016;10:45.
- 5
- 6 **25.** Catafau AM, Bullich S, Seibyl JP, et al. Cerebellar amyloid-beta plaques:
7 How frequent are they, and do they influence 18F-Florbetaben SUV ratios? *J*
8 *Nucl Med.* 2016;57:1740-1745.
- 9
- 10 **26.** Blume T, Focke C, Peters F, et al. Microglial response to increasing
11 amyloid load saturates with aging: a longitudinal dual tracer in vivo muPET-study.
12 *J Neuroinflammation.* 2018;15:307.
- 13
- 14 **27.** Ulrich JD, Ulland TK, Mahan TE, et al. ApoE facilitates the microglial
15 response to amyloid plaque pathology. *J Exp Med.* 2018;215:1047-1058.
- 16
- 17 **28.** Brendel M, Kleinberger G, Probst F, et al. Increase of TREM2 during
18 aging of an Alzheimer's disease mouse model Is paralleled by microglial
19 activation and amyloidosis. *Front Aging Neurosci.* 2017;9:8.
- 20
- 21 **29.** Foley AM, Ammar ZM, Lee RH, Mitchell CS. Systematic review of the
22 relationship between amyloid-beta levels and measures of transgenic mouse
23 cognitive deficit in Alzheimer's disease. *J Alzheimers Dis.* 2015;44:787-795.

1

2 **30.** Focke C, Blume T, Zott B, et al. Early and longitudinal microglial activation
3 but not amyloid accumulation predict cognitive outcome in PS2APP mice. *J Nucl*
4 *Med.* 2019;60:548-554.

5

6 **31.** Deleye S, Waldron AM, Verhaeghe J, et al. Evaluation of small-animal
7 PET outcome measures to detect disease modification induced by BACE
8 inhibition in a transgenic mouse model of Alzheimer disease. *J Nucl Med.*
9 2017;58:1977-1983.

10

11 **32.** Meier SR, Syvanen S, Hultqvist G, et al. Antibody-based in vivo PET
12 imaging detects amyloid-beta reduction in alzheimer transgenic mice after BACE-
13 1 inhibition. *J Nucl Med.* 2018;59:1885-1891.

14

15

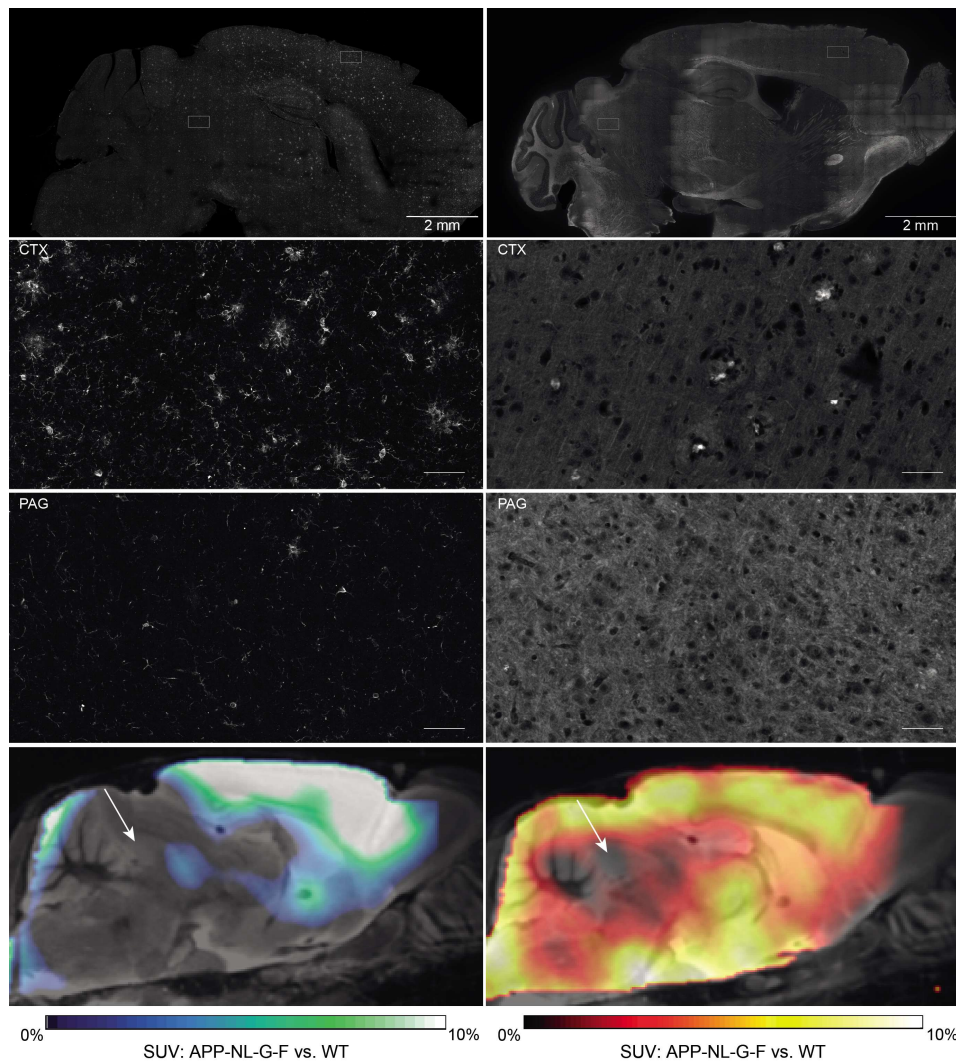


Figure 1: Immunohistochemistry reveals lowest microglia activation (left, Iba-1) and amyloid deposition (right, methoxy-X04) in the periaqueductal gray (PAG) of *App*^{NL-G-F} mice aged ten months (overview and zoom in the upper three panels). Suitability of the PAG as a pseudo-reference tissue was further assessed by comparing SUV of TSPO- and A β -PET images between genotypes (overview in the lowest panel).

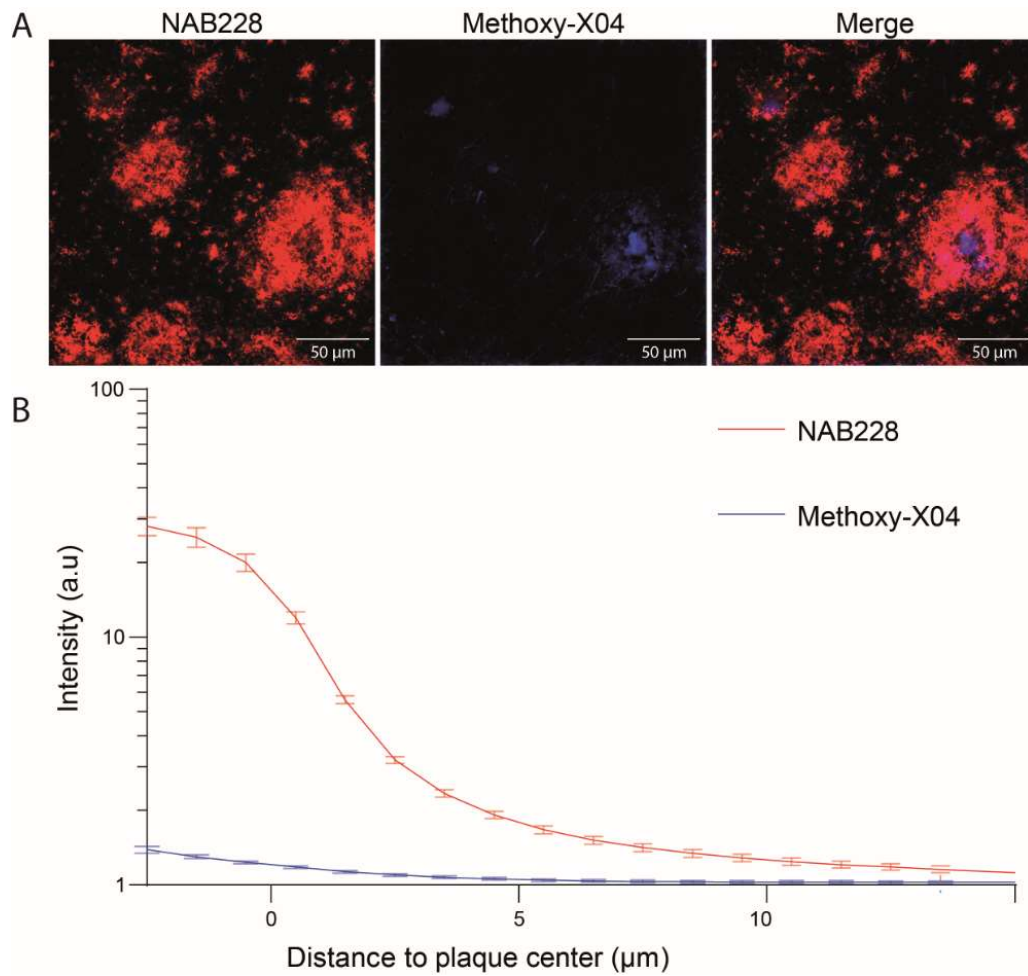


Figure 2: Minor dense fraction of cortical β -amyloid plaques in *App*^{NL-G-F} mice as assessed by NAB228 (red) and methoxy-X04 (blue) co-staining. The graph indicates mean Methoxy-X04 and NAB228 fluorescence intensity profiles from the plaque border; two-way ANOVA interaction staining x distance $F_{(43,704)}=14.79$, $p<0.001$. Data presented as mean \pm SEM with *** $p<0.001$; $n=9$ mice per group; minimal plaque number analyzed per mouse: 41.

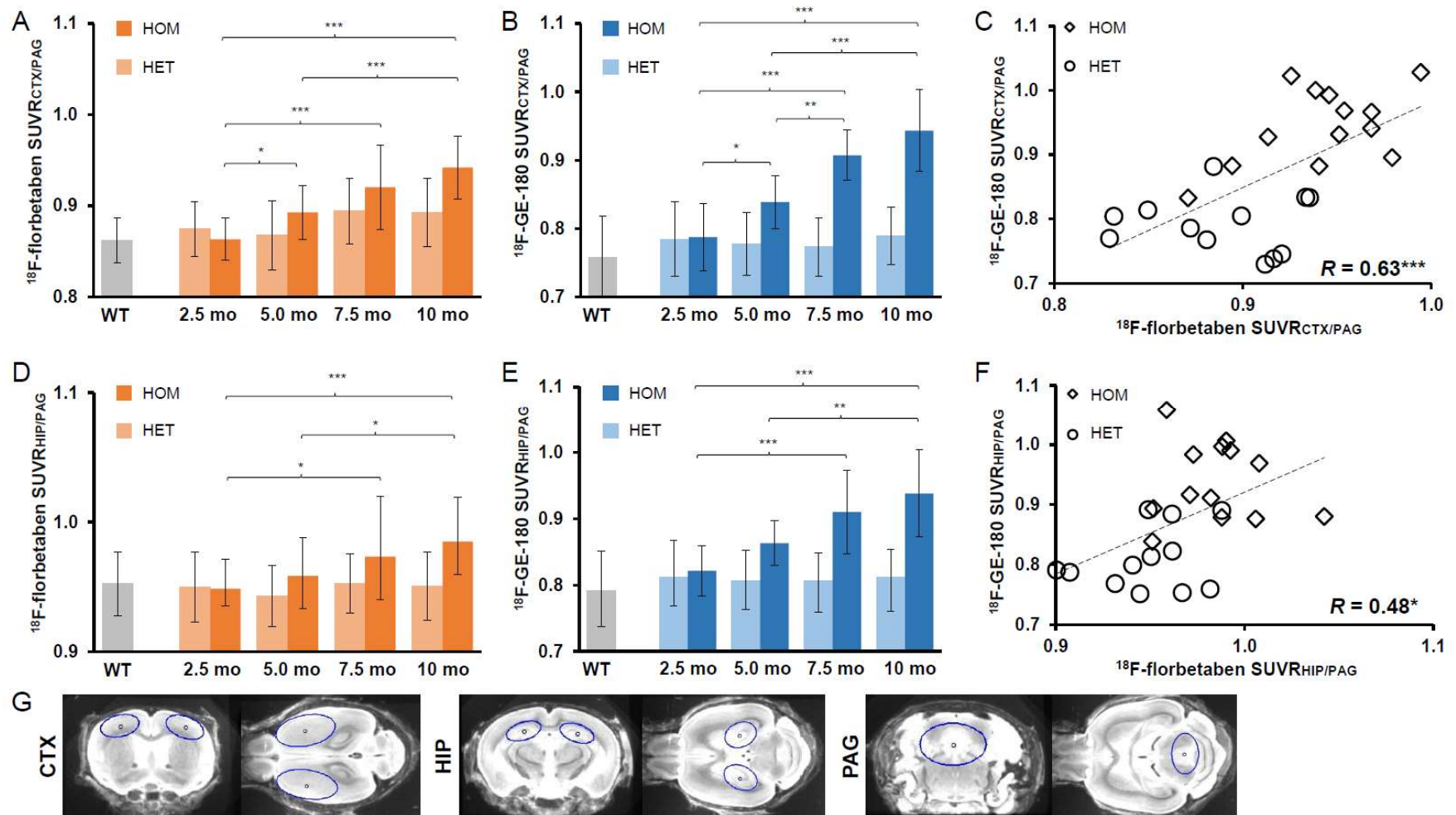


Figure 3: (A,B,D,E) Age dependence of A β and TSPO radiotracer uptake in the frontal cortex and in the hippocampus of homozygous (HOM) and heterozygous (HET) *App*^{NL-G-F} mice. Group comparisons of VOI-based μ PET results between knock-in mouse groups were assessed by one-way ANOVA and Tukey *post hoc* test. (C,F) Correlation between A β -deposition and microglial activation in the frontal cortex and in the hippocampus measured by dual tracer μ PET (R indicate Pearson's coefficients of correlation). * $p < 0.05$; ** $p < 0.01$; *** $p < 0.001$. (G) Definitions of cortical (CTX), hippocampal (HIP) and periaqueductal gray (PAG) VOIs in coronal and axial slices upon an MRI mouse brain atlas.

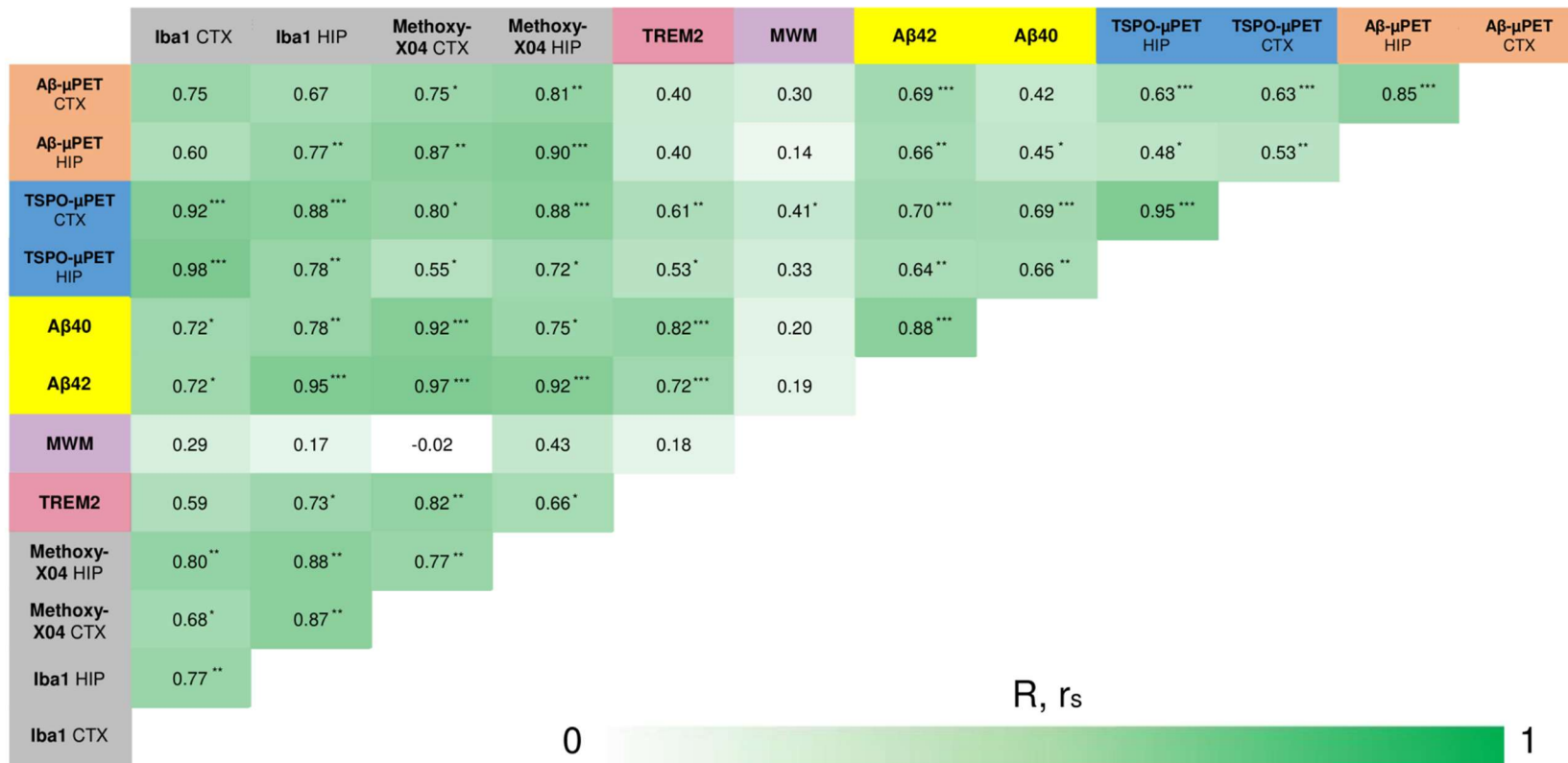


Figure 4: Correlation analyses of all terminal readouts. Pearson's coefficients of correlation (R) were calculated for normally distributed readouts (μPET, behaviour, Iba1, methoxy-X04). For the remaining not normally distributed readouts, Spearman's coefficients of correlation (r_s) were calculated. *p<0.05; **p<0.01; ***p<0.001

Table 1: Overview of μ PET results

Group	Age			Amyloid-μPET		TSPO-μPET			
	months	n	sex	Cortex (SUVR)	Hippocampus (SUVR)	n	sex	Cortex (SUVR)	Hippocampus (SUVR)
<i>App</i> ^{NL-G-F} (homozygous)	2.5	20	9♂/11♀	0.86±0.02	0.95±0.01	18	9♂/9♀	0.79±0.05	0.82±0.04
	5.0	17	6♂/11♀	0.89±0.03*	0.96±0.02	17	6♂/11♀	0.84±0.04*	0.86±0.03
	7.5	13	6♂/7♀	0.92±0.05***	0.97±0.03*	14	6♂/8♀	0.91±0.04***	0.91±0.06***
	10	13	6♂/7♀	0.94±0.03***	0.98±0.02***	13	6♂/7♀	0.94±0.06***	0.94±0.07***
<i>App</i> ^{NL-G-F} (heterozygous)	2.5	21	13♂/8♀	0.87±0.03	0.95±0.03	20	12♂/8♀	0.78±0.06	0.81±0.04
	5.0	20	12♂/8♀	0.87±0.04	0.94±0.02	20	12♂/8♀	0.78±0.05	0.81±0.04
	7.5	15	9♂/6♀	0.89±0.04	0.95±0.02	17	10♂/7♀	0.77±0.04	0.81±0.05
	10	13	8♂/5♀	0.89±0.04	0.95±0.03	13	8♂/5♀	0.79±0.04	0.81±0.05
C57BL/6 (wild-type)	2.5	6	3♂/3♀	0.87±0.03	0.96±0.01	6	3♂/3♀	0.75±0.07	0.80±0.04
	10	6	3♂/3♀	0.86±0.01	0.95±0.01	6	3♂/3♀	0.82±0.04	0.84±0.03

P-values for one-way ANOVA including *post-hoc* Tukey testing versus baseline given by: * $p < 0.05$; *** $p < 0.001$. Numbers (n) of mice included in PET analyses by sex are provided for each tracer and age.

Voxel-wise Analyses

Results

Voxel-wise group contrasts between knock-in and WT animals are shown in Supplemental Fig. 3. By this exploratory approach, the strongest differences in ^{18}F -FBB uptake between homozygous *App*^{NL-G-F} and wild-type mice ($p < 0.001$, unc.) were discerned in the left thalamus. This first became apparent at five months, whereas comparable thalamic elevations in the heterozygous genotype emerged only at 7.5 months. Significant SUVR increases in neocortical areas were observed in homozygous *App*^{NL-G-F} mice only at ten months of age, when 29% of the total brain volume had elevated ^{18}F -FBB signal relative to the wild-type group.

Voxel-wise TSPO- μ PET analysis revealed microglial activation in homozygous *App*^{NL-G-F} mice in the frontal cortex and the hippocampus starting at five months (18% of total brain volume, $p < 0.001$, unc.), which increasing to involvement of 48% of total brain volume at ten months of age ($p < 0.001$, unc.), including thalamic regions. heterozygous *App*^{NL-G-F} animals showed no differences of ^{18}F -GE-180 uptake relative to WT at any age.

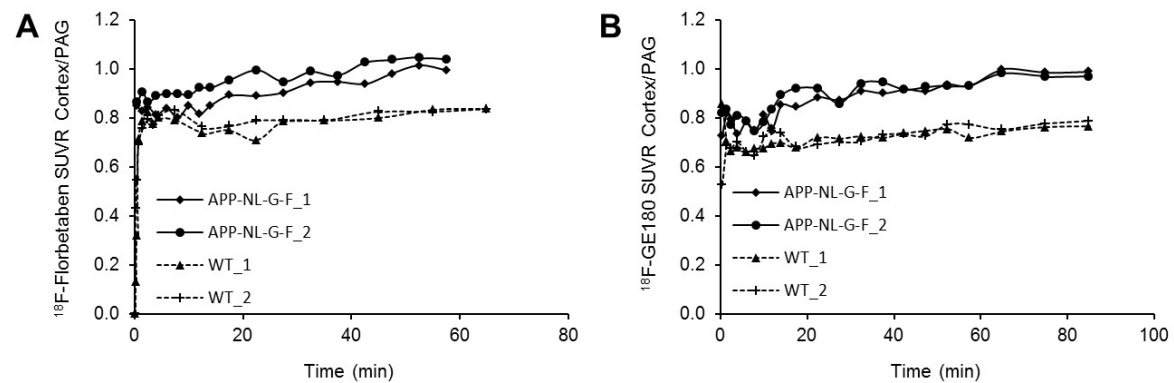
Discussion

Voxel-wise group contrasts between knock-in and WT animals revealed increased ^{18}F -FBB uptake in homozygous *App*^{NL-G-F} mice already at five months of age. Notably, early increases in amyloid binding were present in thalamus of homozygous and heterozygous *App*^{NL-G-F} animals. This finding in thalamus of knock-in mice is in contrast to sporadic AD, and thalamus is not typically considered a target region for therapy studies in AD mouse models.

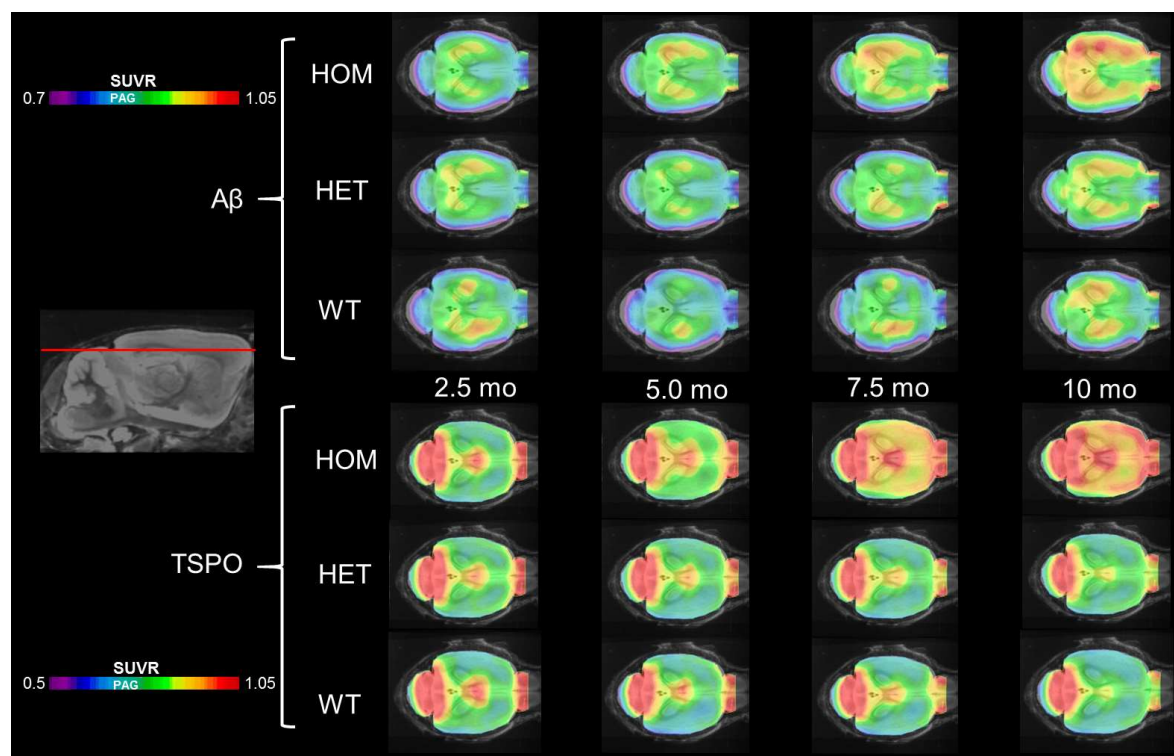
Spatial learning

Discussion

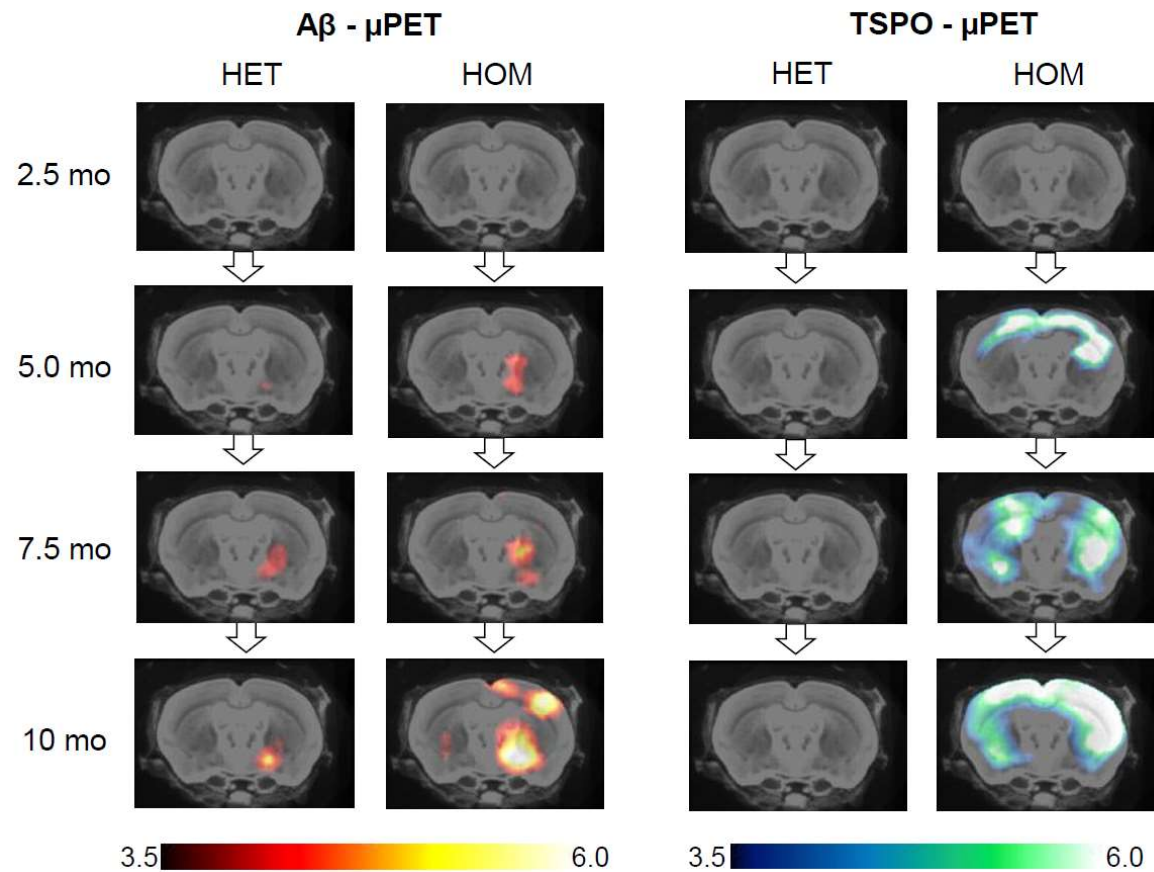
Recent publications report that homozygous *App*^{NL-G-F} mice show subtle, progressive deterioration in performance of spatial learning trials, deficits in flexible learning, and reduced attentional performance compared to wild-type (see reference 10 of the manuscript). Consistent with these findings, we observed a significant deficit in spatial learning in homozygous *App*^{NL-G-F} mice in performing the hippocampus-related Morris water maze test. However, the learning and memory deficits in *App*^{NL-G-F} mice should be further investigated since another study has reported intact learning and memory in homozygous *App*^{NL-G-F} aged as much as 15-18 months (see reference 12 of the manuscript)



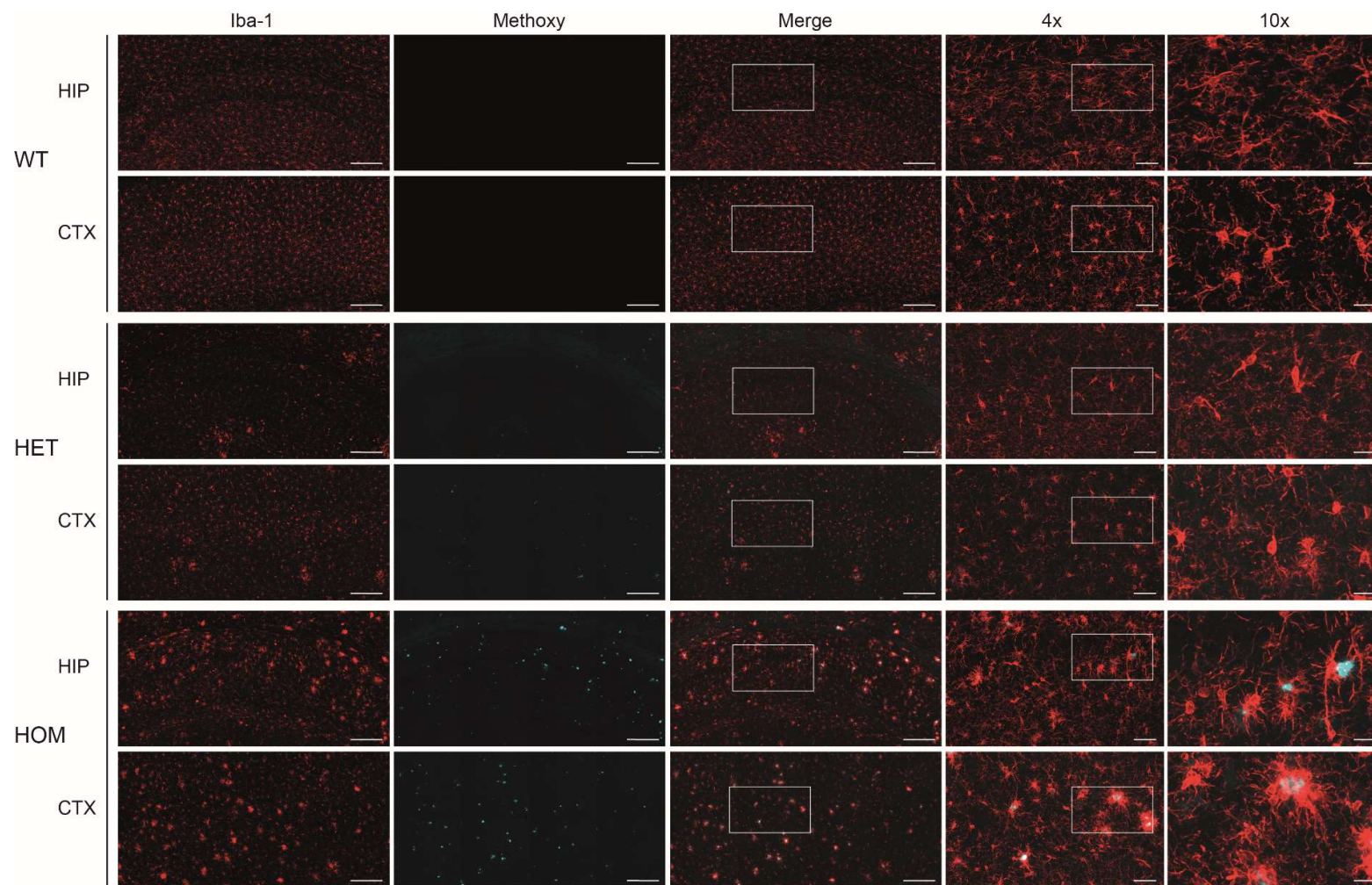
Supplemental Figure 1: Dynamic PET imaging of *App*^{NL-G-F} mice with ¹⁸F-florbetaben (**A**; 0-60 min p.i.) and ¹⁸F-GE-180 (**B**; 0-90 min p.i.). Time-activity-curves show ratios of the cortical target region divided by the periaqueductal grey (PAG) for two *App*^{NL-G-F} mice and two historic wild-type (WT) mice.



Supplemental Figure 2. Mean parametric SUVR images in axial planes of the A β tracer ^{18}F -FBB and the TSPO tracer ^{18}F -GE-180 at different ages of HOM and HET *App*^{NL-G-F} and pooled WT mice projected on MRI mouse atlas.



Supplemental Figure 3: Voxel-wise group comparisons of Aβ and TSPO radiotracer uptake of homozygous (HOM) and heterozygous (HET) *App^{NL-G-F}* mice versus age-matched WT mice at different ages. Two-sample t-test, $p < 0.001$ uncorrected for multiple comparisons, $k > 20$ voxels, projected upon an MRI mouse atlas (coronal slices).



Supplemental Figure 4. Representative immunohistochemical (Iba-1) images of microglial activation and histochemical images showing and fibrillar A β (Methoxy-X04), as well as merged images in cortical (CTX) and hippocampal (HIP) target regions for wild-type (WT) and heterozygous (HET) and homozygous (HOM) *App*^{NL-G-F} mice. Scale bars represent 200 μ m (columns 1-3), 50 μ m (column 4) and 20 μ m (column 5).

Supplemental Table 1: Overview of multimodal terminal readouts

Group (Age=10mo)	Biochemistry			Histochemistry				Behavior Latency to platform (s)
	A β 40 (μ g/g)	A β 42 (μ g/g)	sTrem2 (ng/g)	Methoxy-X04 CTX (%)	Methoxy-X04 HIP (%)	Iba1 CTX (%)	Iba1 HIP (%)	
<i>App</i> ^{NL-G-F} (homozygous)	0.3 \pm 0.1*** n=8	96.9 \pm 23.7*** n=8	39.5 \pm 4.7*** n=8	1.3 \pm 0.3** n=4	1.4 \pm 0.1*** n=5	8.5 \pm 2.2* n=5	10.0 \pm 2.0*** n=5	29.4 \pm 16.8* n=11
<i>App</i> ^{NL-G-F} (heterozygous)	<0.1 n=14	17.6 \pm 4.6 n=14	11.7 \pm 2.3 n=14	0.4 \pm 0.3 n=5	0.1 \pm 0.1 n=5	5.1 \pm 1.3 n=5	3.3 \pm 1.1 n=5	20.1 \pm 11.7 n=14
C57BL/6 (wild-type)	<0.1 n=4	0.3 \pm 0.2 n=3	9.5 \pm 1.7 n=4	not detected	not detected	4.3 \pm 0.9 n=4	2.4 \pm 0.8 n=4	14.3 \pm 4.7 n=3

A β and sTrem2 levels are given as ng per g of wet brain tissue. P-values for two-sided t-test in the comparison of homozygous *App*^{NL-G-F} versus wild-type are given by: *p<0.05; **p<0.01; ***p<0.001; two-tails. Methoxy-X04 staining of homozygous *App*^{NL-G-F} was tested against heterozygous *App*^{NL-G-F} due to no detectable A β plaques in wild-type. Histology quantification: 3-dimensional 16-bit data stacks of 8192x4096x32 pixels of confocal microscope images were acquired for the whole cortex as well as hippocampus at a lateral resolution of 0.2 μ m/pixel and an axial resolution of 1.0 μ m/pixel. To quantify Iba1-positive microglia burden as well as plaque-load we used autothresholding in ImageJ. For staining of fibrillar plaques we acquired 3-dimensional 16-bit data stacks of 2048x2048x120 pixels from five different positions in the frontal cortex as well as hippocampus at a lateral resolution of 0.17 μ m/pixel and an axial resolution of 0.4 μ m/pixel. For plaque quantitation, we utilized custom-written Matlab software (MathWorks, Natick, USA).

Supplemental Table 2: Comparison between mouse models

Mouse model	Onset of congophilic Amyloidosis (months)	Age range of PET imaging (months)	Reference tissue	Amyloid μ PET (Cortical Increase)	TSPO μ PET (Cortical Increase)	Correlation sTrem2 - Amyloid- μ PET (terminal)	Correlation sTrem2 - TSPO- μ PET (terminal)	Correlation Water maze - Amyloid- μ PET (terminal)	Correlation Water maze - TSPO- μ PET (terminal)
<i>App</i> ^{NL-G-F}	2.0	2.5-10.0	PAG	9.1%	19.8%	-	++ (pos.)	-	+ (pos.)
PS2APP (16)	5.0	5.0-16.0	WM	19.8%	20.2%	+++ (pos.)	+++ (pos.)	-	++ (neg.)
APP-SL70 (26)	5.0	5.5-12.5 (average)	WM	18.3%	17.6%	n.a.	n.a.	n.a.	n.a.

Overview of findings in homozygous *App*^{NL-G-F} mice compared to other AD model mouse strains investigated with comparable μ PET modalities. For comparing the correlations, we indicate significant R/ r_s by + (0.2-0.5), ++ (0.5-0.8), +++ (0.8-1.0). n.a. = not assessed